Original Research Article

Geochronology of Recent Sediments from the Upper Bonny Estuary (Niger Delta) Using Naturally Occurring Radionuclides

ABSTRACT

The research evaluated temporal trends of naturally occurring radionuclides and their vertical distributions in sediment cores collected from three sites of diverse sedimentation regimes in Bonny Estuary, and developed and implemented sediment dating with unsupported lead-210.The temporal variations of Radium (Ra) isotopes showed a fairly uniform distribution among all sampled cores in each month with ^{228}Ra, while ^{226}Ra displayed some variability with generally lower specific activities in dry months than in wet months. The values found in the study were all less than unity ranging from 0.3 to 0.8, which suggested sediment accretion and that the study area corresponded to zones with different sedimentation regimes. Temporal distribution of total ^{210}Pb in the sampled cores determined via its daughter ^{210}Po by alpha spectrometry assumed that the secular equilibrium between both radionuclides was achieved. However, the activities in Station 3 were found to be lower than those in Station 1, with Station 2 having the lowest activity registered in the samples collected in December month. The specific activities of ^{228}Ac (^{228}Ra), ^{212}Pb (^{228}Th) and ^{40}K against depth in the sampled cores were observed to be almost equal to one another at each stratigraphic interval. The average sedimentation rate throughout the core obtained from Constant Rate of Supply model (0.068 ± 0.015g.cm^{-2}.y^{-1}) was nearly the same as that obtained from the Constant Initial Concentration model (0.065 ± 0.004). However, the estimated ages were quite variable with depths of various stratigraphic layers. The age of the sediment core was dated approximately 80 years, which was qualitatively validated using ^{137}CS whose activity was definitely undetected in the basal part of the core. The sedimentation rates calculated suggested low sedimentation characterized by low energy environment dominated by weak tidal currents.

Keywords: Sedimentation, Radionuclides, Upper Bonny Estuary, Niger Delta

1. INTRODUCTION

Naturally occurring radioactive materials (NORM) are found almost everywhere. NORM is inherent in many geologic materials and consequently, encountered during geological related activities. NORM encountered in hydrocarbon exploration and production operations originate in subsurface formations that may contain radioactive materials such as uranium and thorium and their daughter products, ^{226}Ra and ^{228}Ra [1, 2].During exploration and extraction processes, various operational practices contribute to or induce NORM occurrence. These include remote sensing methods of mapping and explosives associated with seismic exploration, drilling equipment and activities of downhole geophysical logging methods. In some instances, radioactive marker bullets are employed as an aid in relative depth determinations. The gamma ray log is used to locate the bullets after casing has been set. Radioactive tracers are also used in evaluating the effectiveness of well cementing and underground water and crude oil flow direction for the purpose of correlation [1]. In some cases, various amounts of radioisotopes are injected during secondary recovery operation to facilitate fluid flow.

Lead-210 is a radioisotope, which is a member of the ^{238}U decay series. Uranium-238 has a half-life of 4.5×10^{9} years and decays through several daughters to ^{226}Ra, which has a half-life of 1600 years. Radium-226 in rocks, soil and saltwater decays to radon gas (^{222}Rn, t1/2=3.8 days), some of which escapes to the atmosphere. Radon gas undergoes decay through a series of short-lived daughters to yield particulate ^{210}Pb, which has a half-life of 22.3 years. This ^{210}Pb in the atmosphere can be delivered to the earth via rainfall (washout) or dry fallout [3]. Atmospheric ^{210}Pb is ultimately delivered to water bodies primarily by direct fallout, but a fraction of the unsupported ^{210}Pb that reaches lakes may also be delivered via transport from the watershed.

Lead-210 dating has become a common procedure in paleoenvironmental studies that requires age-depth relationship for sediments deposited over the past 100-150 years [4]. Forty years ago, Goldberg [5] proposed the use of ^{210}Pb as a chronological tool in earth science. Since then, both alpha and gamma counting techniques have been employed to estimate the stratigraphic distribution of ^{210}Pb activity in recent sediments [6,7,8]. Over the same time period, several dating models came into widespread use [9]. In the past four decades or so, thousands of investigations have relied on the approach to develop recent sediment chronologies [10].

The Bonny Estuary (Fig.1), which is the study site, has been the focal point for a wide variety of human activities; including a major sea port, industrial, urban and recreational facilities. It is an important zone of great diversities and sediment transfer, which often form sinks for sediment moving downstream, alongshore or landwards. The research is aimed at determining levels of radionuclides in sediment samples from within the Bonny Estuary, evaluate the temporal trends of naturally occurring radionuclides and their vertical distributions in sediment cores collected from sites of diverse sedimentation regimes in the area, develop and implement sediment dating with the unsupported lead-210, assess the degree of catchment disturbance by comparing recent sedimentation rates with pre-European sedimentation rates.

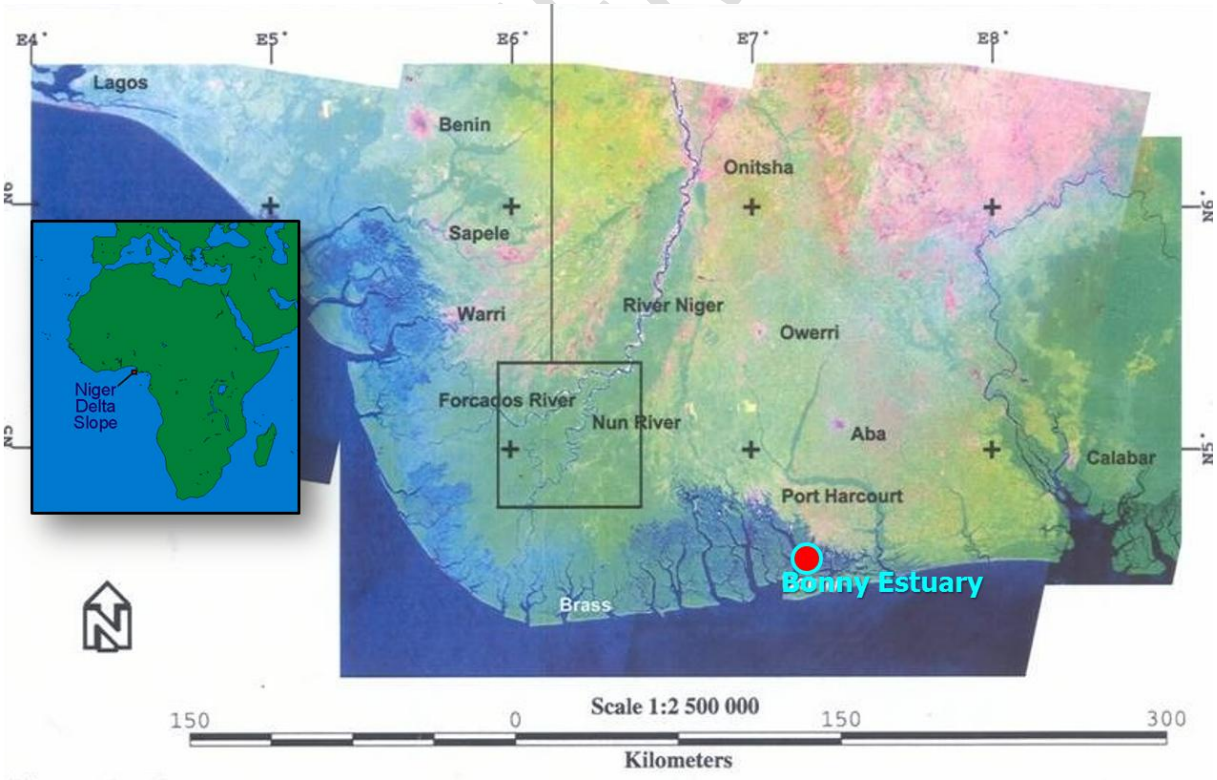

Fig. 1: Satellite Imagery of the Niger Delta showing the Bonny Estuary [11].

1.1 Geology and Physiography of the Niger Delta Coastline

An excellent review of the general geology of the Niger Delta with reference to three aspects of the stratigraphy, sedimentation and structural geology was carried out by Asseez [12]. The formation of the proto Niger Delta started in the Campanian period while the formation of the modern delta was in the Eocene period, about 40 to 63 million years ago (Fig.2). The basin covers about 50% of the total length of the Nigerian Coastline and it is situated in the Gulf of Guinea between longitudes 5^0E and 8^0 E, and latitudes 4^0N and 6^0N. It is the largest wetland in Africa and the third largest in the world consisting of flat low lying swampy terrain that is criss-crossed by meandering and anastomosing streams, rivers and creeks consisting of three major stratigraphic units namely the Benin Formation (consisting predominantly of sandstones), Agbada Formation (consisting of sandstones and shales) and the Akata Formation (consisting of shales) [13].

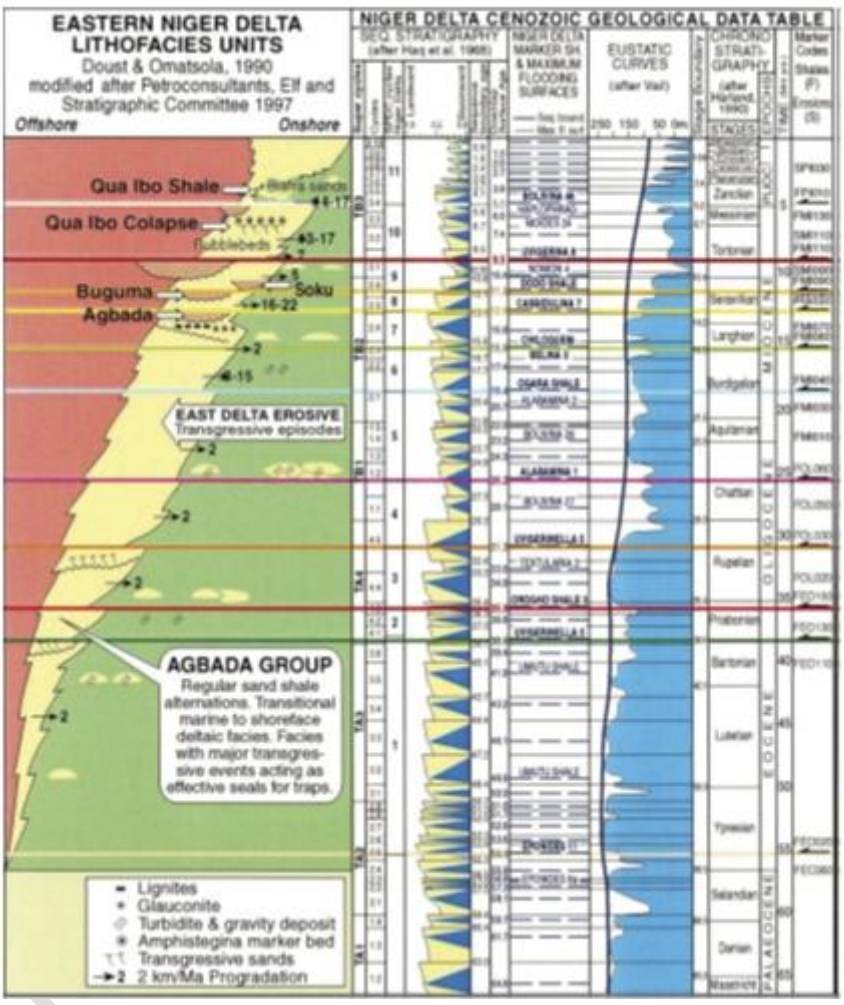

Fig. 2: Stratigraphic Column of the Eastern Niger Delta showing Lithofacies Units and Cenozoic Geological Data [14]

The coastline of the Niger Delta extends from the mouth of the Benin River in the west to the mouth of the Imo River in the east. It has twenty one (21) major channels from the Benin River to the Imo River namely Benin, Escravos, Forcados, Ramos, Dodo, Pennington, Digatoru, Bentagoru, Koluama, Fish Town, Sangana, Nun Brass, St. Nicholas, Santa Barbra, St. Bartholomew, Sombriero, New Calabar, Bonny, Andoni, and Imo Rivers. All of these open into the Atlantic Ocean [15] (Fig.1).

The Bonny River is one of the numerous low land coastal rivers of the Niger Delta basin. It is geographically located between latitudes 4^0 25'N and 4^0 50'N, and longitudes $7^0$00'E and 7^0 15'E in River State, Nigeria. Like most other rivers, it is short, extending approximately 180km from its mouth. It is bordered to the east by tidal divide of the Andoni basin, to the northeast and north by the coastal

plain sands of the river Sombreiro drainage, to the west by tidal waters of the New Calabar River system. The river has a low relief of less than 50km above sea- level [16], and covering a tidal swamp system of about 730.24 ha [17].

The river system of the Bonny Estuary consists of a main river channel and large numbers of associated creeks and creek-lets. It has the largest tidal volume (maximum width of 2km and maximum depth of approximately 15m near the mouth) of all river systems in the Niger Delta and it is mostly affected by tidal movements [15]. This is attributed to its low elevations, easy access for the tidal water into the system, virtual absence of fresh water discharge, and the configuration of the basin which causes the tidal range to increase inland [15,18]. Seasonality is observed in the salinity of the brackish water especially at the limit of salt water intrusion during the wet season; fresh water discharge increases as rain fall increases. This pushes the limit of the salt water intrusion seawards and reduces salinity in the brackish areas.

Generally, the delta is characterised by sandy shorelines backed by extensive mangrove swamps and Barrier Island separated by tidal channels. The region is characterised by semi-diurnal tidal regimes with tidal amplitude of about 1.2m high and ebb flow rates reaching higher velocities than flood flow [15]. It has a unique feature known as the tidal mudflat.

The delta formation is the most important drainage features of the Niger-Benue river system and drains about 60% of Nigeria and about 34% of the entire West Africa [13]. The River Niger which drains a large part of West Africa discharges its waters, sediments and other loads into the Niger Delta and by extension into the Atlantic Ocean.

The hydrology of the delta is dominated by three types of flow namely a unidirectional flow in the upper Niger Delta, a bidirectional tidal flow in the coastal area and estuaries, and a mixed flow in which the uni- and bidirectional attributes are combined in the transitional zone [19]. A typical hydrograph for the upper Niger Delta shows a dry season period of some five months (December-April) followed by a gradual rise in water level, reaching a peak period around September/October. The interior back swamps are frequently flooded before the attainment of peak floods because of their relative low elevation and structural connections to the main drainage channel. The water so accumulated in the back swamps does not often have a way to discharge or drain by gravity because of the very low gradient and permeability of the subsoil. The water level starts falling rather abruptly soon after attainment of peak water stage, reaching its dry season level in less than 45 days. The actual discharge depends on the climatic conditions.

The coastal area of the delta is dominated by a daily rise and fall in water level with a range at spring tide varying from 1.8m to 2.75m in the west and east respectively. The annual rain fall of the Niger Delta is between 2000mm and 3000mm a year and falls mostly during nine months from March to November. Rainfall decreases sharply as one moves inland. The dry season lasts for less than three months from December to February. In these three months, there is an average of 2-3days each month with a rainfall of over 1mm (Port Harcourt Metrological Service).

1.2 Measurement of Radionuclides in Sediments

Unsupported ^{210}Pb activity can be estimated by two methods, alpha or gamma counting. Both approaches require that total ^{210}Pb activity be measured in each stratigraphic sample down to a depth where no measurable unsupported ^{210}Pb remains. Supported ^{210}Pb activity, measured or approximated by an appropriate means, should be subtracted from the total activity to yield an estimate of unsupported ^{210}Pb activity. The alpha and gamma counting methods vary with respect to how total and supported ^{210}Pb activities are assessed. Total ^{210}Pb activity can be measured by alpha counting of the granddaughter radionuclide, ^{210}Po [6]. This method has several advantages. The high sensitivity of alpha detectors make them suitable for counting samples with low activity. Small amounts of sample can therefore be used, which permits high-resolution (i.e. at small depth interval)

counting, even in sediments with low bulk density. Furthermore, alpha detectors are relatively simple and inexpensive [4]. Nonetheless, the alpha counting procedure has several drawbacks. First, samples must be digested in acid and the acid-extracted ^{210}Po must be plated on metal (Ag or Cu) disks. Second, samples are destroyed during this chemical process. Third, the wet chemistry method requires use of a yield tracer (^{208}Po) to access the efficiency of radioisotope plating on the metal planchets. Fourth, topmost sediments should be held for almost 2 years before counting to guarantee that equilibrium between ^{210}Pb and measured ^{210}Po is achieved. Lastly, supported ^{210}Pb activity is not measured directly with alpha counter. Instead, it is generally estimated by the down-core, asymptotic total ^{210}Pb activity has remained unchanged over the past 100-150 years. Less commonly, ^{226}Ra activity is measured by an independent analytical technique, allowing for subtraction of supported ^{210}Pb activity from the total ^{210}Pb activity (i.e.^{210}Po) on a level-by-level basis.

1.3 Application of Radionuclides in Sediment Tracing

Environmental radionuclides refer to radionuclides which commonly occur at low, measurable levels and are widely distributed in the environment including sediments. In most cases they are of natural origin. For applications relating to sediment tracing, most work to date have focused on a particular group of environmental radionuclides, namely *fallout radionuclides*, or radionuclides which reach the land surface as fallout from the atmosphere. The fallout input can generally be assumed to be spatially uniform, at least over a relatively small area. Because the radionuclides employed are rapidly and strongly adsorbed by the sediments on reaching the catchment surface as fallouts, they accumulate at or near the surface and afford a means of tracing sediment mobilization and deposition. The use of fallout radionuclides as sediment tracers has primarily focused on the unsupported or excess lead-210 (^{210}Pb) and ^{137}Cs. Lead-210 differs from ^{137}Cs in two important respects. Firstly, ^{210}Pb is of natural origin, and secondly, their fallout input can be treated as essentially constant over time [20]. Lead-210 is often deployed as a chronological tool while ^{137}Cs as chronological marker, for sediments in conjunction with alpha and gamma counting techniques to estimate the stratigraphic distribution of the activity of radionuclide of interest.

Regardless of how ^{210}Pb in sediments is measured or what dating model is chosen, application of the method depends on accurate estimation of unsupported (i.e. excess or atmospherically derived) ^{210}Pb activity at contiguous depths throughout the upper portion of a sediment core. Presence of supported ^{210}Pb in sediments complicates the dating procedure. Atmospherically derived (unsupported or excess) ^{210}Pb must be distinguished from supported ^{210}Pb, which is produced by decay-series precursor within or attached to the sediment matrix. Supported ^{210}Pb activity assumed to come from in situ ^{226}Ra, with which it is generally believed to be in secular equilibrium. The ^{226}Ra in the sediments typically comes from local soil and bedrock particles, which are delivered to the lake by colluviation, alleviation, or aeolian transport.

1.4 Biological Influences on Sediment Homogeneity

Sediment systems support a large number of organisms and the activities of these organisms have a large influence upon the overall sediment homogeneity. Almost every organism inhabiting sediments will interact with their environment; directly changing the characteristics of the sediment. The consequences of such actions on sediment homogeneity are highly variable, and research on the influences of individual species is extensive. Widdows and Brinsley [21] divided macro fauna species into two functional groups; sediment stabilisers or destabilisers (bio-stabilisers and bio-destabilisers). Possibly, included within stabilisers could be bio-depositors, species that increase deposition rates of suspended particles [22]. Bioturbation can as well disrupts the sediment, usually leaving it less consolidated and increasing its surface roughness, there by generally reducing its critical erosion threshold [23, 24]. The methods through which species interacts with the sediment are highly variable but can usually be placed into one of several categories.

1.5 Sediment Yield and Transport

Sediment systems in watersheds not only cause sediment yield but also sediment transportation along rivers. Sediment yield is the amount of sediment passing through a specified channel and location that may be influenced by a number of geomorphic features and processes. It may be substantially less than the amount eroded in the basin. Sediment yield is typically expressed as the total sediment volume delivered to a specified location in the basin divided by the effective drainage area above the location for a specified period of time. Yield typically has the units of cubic meters/square kilometre/year [25].

Sediment transport on the other hand is the movement of solid particles (sediment) typically due to a combination of force of gravity acting on the sediment and/or the movement of the fluid in which the sediment is entrained. Sediment transport due to fluid motion occurs in rivers, oceans and lakes due to currents and tides. Knowledge of sediment transport is most often used to know whether erosion or deposition will occur, the magnitude of the erosion or deposition, and the time and distance over which it will occur [26]. In Nigeria, sediments transported to the Niger Delta basin are derived from seven of the eight hydrological provinces of Nigeria namely Niger North, Niger Central, Upper Benue, Lower Benue, Niger South, Western Littoral, Eastern Littoral and Lake chad. These seven provinces have a combined catchment area of 1413986 km" and reservoir capacity of 29578.7 million m^3. A total of 135 small, medium and large dams and reservoirs are located within the seven hydrological zones impacting directly on the Niger Delta.

The combined effect of reservoir sediment impoundment and increased in-channel sedimentation is a reduction in the sediment load of coast bound waters. Given that historical records of discharge distribution to the east and west delta indicates 55% preference for the western delta, it is expected that sediment delivery to the coast of the western delta would be significantly higher. This skewed distribution was also maintained during the period 1983-1984, which happened to be that of a very severe drought in the Sahel and the Sudan, when the lowest flow volumes in 40 years were recorded. Although significantly higher, the sediment delivered to the western delta has not been sufficient in sustaining accretion in the area. This is evident from a comparison of satellite imageries of the coastal area between 1963 and 1988, around two strategic river estuaries, which together control 30%o of the Niger River discharge, namely, the Forcados and Ramos rivers .The significant coastline recessions revealed in this is strong evidence of the large sediment impoundment of dams, particularly Kainji which was commissioned in 1968.

Indeed recent investigations by Ibe, [27] have revealed a net retreat of the coastline in the eastern section of the Niger Delta and only marginal accretion in limited sections of the western Niger Delta. The net erosion of the eastern coastline is explained by its non-direct connection to the Niger-Benue River system that conveys the bulk of the sediments. Furthermore, the drainage rivers in the eastern delta have limited extent and catchment size in comparison to their western counterparts. The erosion stress being experienced at the coast presently will gain further strength with the anticipated rise in mean sea level because of the associated stronger coastal hydraulic forces. These patterns of coastline development contrast with an earlier report which reflected the pre-Kainji dam status and suggested a strong erosion stress and a shift in the existing ecological balance. The presence of strong erosion stress suggested that there is not enough sediment reaching some sections of the coast to sustain the existing ecological balance between coastal erosive processes and constructive hydrological processes.

The dams have gradually silted up with the continuous entrapment of sediments, thus decreasing their capacity to impound water. Consequently, the dams are no longer able to function effectively as flow buffers. Floods in the downstream locations are therefore expected to increase towards pre-dam levels, except when dam reservoirs are dredged to increase their holding capacity. Water levels which depressed following intensive dam construction between 1968 and 1985 are beginning a modest upward trend. Flooding was particularly severe in 1988 and 1994, forcing people to seek shelter on

higher grounds; leaving crops and houses to be destroyed. However, the new flood water carries only little or no sediments compared with the pre-dam years.

1.6 Sediment Dating Models

Two ^{210}Pb dating models have come into general use. The constant initial concentration (CIC) model, which assumes that lake water has a substantial reservoir of excess of unsupported ^{210}Pb. According to this model, the water column contains abundant ^{210}Pb, regardless of the bulk sediment accumulation rate. Sediment scavenging of the radioisotope is proportional to the rate of sediment deposition, which precedes in such a manner that surface sediments always have the same initial activity – hence the model name. The other model is constant rate of supply (CRS) model, which assumes that the input of excess ^{210}Pb to the sediments has remained constant through time. Under this scenario, high rate of bulk sediment accumulation dilute incoming excess ^{210}Pb, yielding low activities in deposits. Conversely, slower bulk sedimentation rates result in relatively higher ^{210}Pb activities in the accumulating sediment [28].

2. Materials and Methods

2.1 Experimental Design

Both field and laboratory investigations were conducted bi-monthly for a total of eighteen months and sampling covered both wet and dry seasons. Before commencement of the experiment, three sampling locations were established at 1000m intervals in a relatively undisturbed sections of the river (Fig.1). Sediment cores and surface deposits were retrieved from shallow marginal areas at the three stations belonging to the upper Bonny Estuary in 2011/2012 using an Uwitec gravity corer of 10cm internal diameter. During sampling, the sediment remained totally undisturbed in other to obtain the best possible dating. Subsequently, the cores were transported to the laboratory and cut into slices of approximately 2cm, dried and ground, whereupon the content of water and organic matter were determined.

Furthermore, the vertical profiles of ^{226}Ra, ^{210}Pb and its daughter nuclides (^{210}Bi and ^{210}Po, ^{214}Pb, ^{228}Ac, ^{208}Ti amongst orders) activities were determined by alpha and gamma detection. The total hydrocarbon content and total phosphorus down the core were also determined while the temporal and spatial distribution of ^{210}Pb, ^{232}Th and ^{238}U daughters were determined for sub-surface sediment samples collected. The fluxes of ^{210}Pb were used to determine the ages of sediment, sedimentation and accumulation rates while ^{137}Cs was used as chronological markers for the validation of ^{210}Pb dates.

2.2 Field Mapping and Sample Collection

A total of three locations were visited and samples collected at 1000meters intervals along the Bonny River. Sample Station **1** is geographically located between latitude 4°45'04.03"N and longitude 7°00'14.08"E along the downstream section of the Bonny River system. The sampled point is between the Nembe waterside and the dock compound of the Ibeto cement bagging factory.

Sample Stations **2** and **3** are located between latitudes 4°44'12.21"N and 4°46'33.73"N, and longitudes 7°00'01.15"E and 7°00'18.85" respectively along the upstream section of the Bonny River system (Fig.3). The sampled points are at the wharf of the Nigerian Ports Authority (Station **3**) and at a point close to the oil terminal (Station **2**). Nevertheless, both locations receive refinery effluents, which passes through the dug-in channels from petroleum tank farm to the discharge points into the Bonny River.

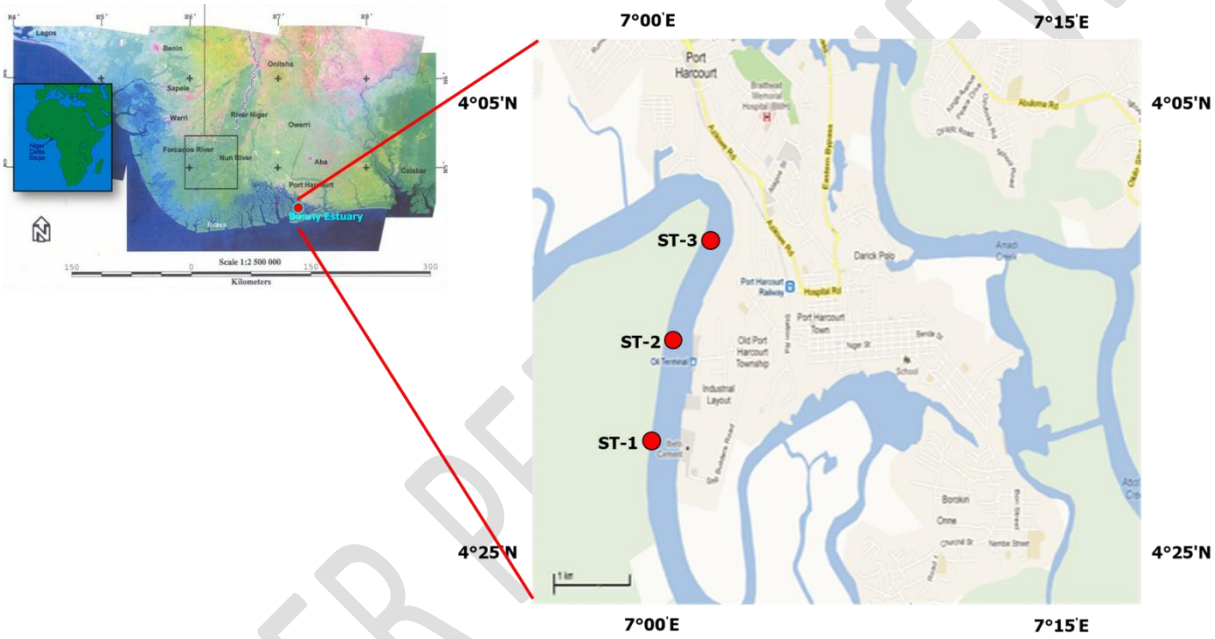

Fig.3: Enlarged Aerial Map of Bonny Estuary showing Sample Stations

The sediment cores were retrieved from shallow marginal areas at the three stations in 2011 using an Uwitec gravity corer of 10cm internal diameter. Thirty-two (32) cm and 30 cm cores were taken from station 1 (St-1) and station 2 (St-2) respectively, while the core from station 3 (St-3) was only 20 cm deep. In addition, sediment surface samples (6cm depth) were also collected from the three stations during different months (August, October, December, February, April and June) covering wet and dry seasons.

The cores were transported immediately after retrieval to the laboratory for pre-treatment and conditioning prior to radiometric analyses. Each core was sectioned into 2-cm slices and wet sub-samples were weighed and then dried using a constant temperature drying oven (24 h at 80°C). Dry samples were weighed again and the content of water in each stratigraphic level was calculated for the three cores. Bulk densities were determined from water content of each slice. Finally, dried sediments were ground in a mortar to fine powder for subsequent alpha and gamma analyses.

2.3 Radiochemical Analyses of Sediment Cores

i. Radionuclides by Alpha Spectrometry

In alpha spectrometry, total ^{210}Pb activity was measured by alpha counting of the daughter radionuclide ^{210}Po. The radiochemical procedure for the determination of ^{210}Po in sediment was based on the isolation of Po from the other elements by self-deposition on silver disc. The deposition was very specific and was carried out in the presence of many other radionuclides in the order of the following procedures:

a. A known amount of dried sample was weighted in a glass beaker and the addition of a weighed aliquot of polonium tracer (^{208}Po or ^{209}Po).
b. Samples were digested using concentrated acids (HNO_3 and HCl).
c. The residue was dissolved in HCl and evaporated to near dryness and further dissolved in about 40 ml of HCl 0.5N
d. The solution was transferred to a 100 ml beaker
e. Subsequently, the original beaker was rinsed with HCl 0.5N and transferred to the solution (making a total volume of 80 ml).
f. A silver disc coated on one side with heat-resistant tape was placed in the bottom of the beaker.
g. The solution was placed on a hot plate at a temperature of about 80°C and stirring was carried out occasionally.
h. After about 6 hours, the disc was removed from the solution and rinsed with H_2O and ethanol and was allowed to dry. The Po source was ready to be counted in an alpha spectrometer.

ii. Radionuclides by Gamma Spectrometry

The outstanding advantage of gamma-ray spectrometry is the ability to measure emitters directly in the original sample without the need for chemical separation. Gamma emitting radionuclides [^{228}Ac (^{228}Ra), ^{214}Bi (^{226}Ra), ^{212}Pb (^{228}Th) and ^{40}K] were measured using a CANBERRA high-purity germanium gamma-ray spectrometer. The relative efficiency was 30% and the resolution was 2 keV for the 1332 keV ^{60}Co γ-peak. Weighed samples were introduced into 20 ml nalgene containers and sealed to trap the gaseous ^{222}Rn and ^{220}Rn emanating from *in-situ* ^{226}Ra and ^{224}Ra, respectively. The flasks were stored for more than 21 days before counting. In some cases, and due to the small quantities of sediment in the upper layers of each core, we combined two to three adjacent sub-samples to reach the working geometry.

^{226}Ra was obtained from ^{214}Bi photopeak at 609.3 keV. Due to the low activity of ^{137}Cs and the low amounts of sub-samples (around 20 g), a detector of HPGe of relative efficiency 70% was used for determination of this radionuclide in each stratigraphic level. The specific activity (in Bq.kg^{-1}) in each sample of all the radionuclides studied was determined from the detector efficiency, gamma intensity and sample weight. The analytical procedure was checked using reference material (IAEA-327). Good agreement was found with certified values, > 90% in all cases.

2.4 Determination of Geoaccumulation Index

The geoaccumulation index (*Igeo)* values were calculated for the different metals as described by Muller [29] as follows**:**

$$I_{geo} = \log_2 \left(\frac{Cn}{1.5xBn!} \right) \quad \text{.....equ1}$$

Where:
Cn= the measured concentration of element 'n' in the sediment
B= the geochemical background for the element 'n'
1.5= is possible variations of the background [30]

However, Muller [29] proposed seven grades or classes of geo-accumulation index**:**

Class 1
Practically uncontaminated = I_{geo}< 0 Class 1
Uncontaminated to moderately contaminated =0< I_{geo} < 1;

Class 2
Moderately contaminated = 0 < I_{geo} < 2;

Class 3
Moderately to heavily contaminated = 2 < I_{geo}< 3;

Class4
Heavily contaminated = 3 < I_{geo}< 4;

Class 5
Heavily to extremely contaminated = 4 < I_{geo}< 5;

Class 6
Extremely contaminated = 5 < $I_{geo.}$

Class 6 is an open class and comprises all values of the index higher than class 5. The elemental concentrations in class 6 may be hundred fold greater than the geochemical background value.

2.5 Sedimentation Rate Modelling

i. Constant Initial Concentration Model (CIC)

The CIC model which assumed a constant ^{210}Pb flux into the sediment and constant sedimentation rate was applied using the formula below:

a. $A = Aoe^{\lambda t}$ ……*equ2*
b. $A = Aoe^{\lambda (x/s)}$ ……*equ3*
c. $\ln A = -(\lambda/S)x + \ln Ao$ ……*equ4*

Where:
A = activity of excess Pb-210 in the sediment at any depth
Ao= Activity of excess Pb-210 in freshly deposited sediment at depth =0(the sediment-water interface)
S= Sedimentation rate in cm /year
λ= Radioactive decay constant (0.0311/year)
t= Time in year
x = excess used

ii. Constant Rate of Supply Model (CRS)

The CRS which takes care of the nonlinear situation of the sedimentation rate but still assumes constant rate of ^{210}Pb fluxes was applied using the total inventory of the ^{210}Pb excess as in the formula below**:**

$S = Ao/Ax*\lambda x$ ……*equ5*

Where:
S= Sedimentation rate
Ao= total ^{210}Pb inventory
Ax= activity of excess ^{210}Pb at any depth x
λ = Radioactive decay constant (0.0311/year)

2.6 Statistical Analysis

The data collated were analyzed statistically using statistical analysis software ANOVA to obtain the mean, standard deviation, error range and statistical differences of ($P<0.05$).

3. RESULTS AND DISCUSSION

i. Temporal Trends of ^{226}Ra and ^{228}Ra in Surface Sediment

The data obtained for radionuclides are presented in figure 4 below, it illustrates the temporal variations of Ra isotopes (^{226}Ra and ^{228}Ra). ^{226}Ra values, which ranged from > 15.67 ± 3.05 to < 34.06 ± 3.61 Bq.kg^{-1} dry weight for all stations during wet and dry seasons while ^{228}Ra were ranged > 33.54 ± 2.64 and < 47.78 ± 2.82 Bq.kg^{-1} dry weight for all station during wet and dry seasons.

The temporal variations of Ra isotopes (^{226}Ra and ^{228}Ra) showed a fairly uniform distribution among locations and months (within error range) with ^{228}Ra, while ^{226}Ra displayed some variability with generally lower specific activities in dry months than in rainy months. The behaviour of these two radioisotopes of radium in estuarine sediment is known to be quite different [31]. Indeed, ^{228}Ra can be more easily desorbed from particles than ^{226}Ra so that the mobility of the former should be lesser than that of ^{228}Ra. Furthermore, ^{226}Ra to ^{228}Ra ratios were also investigated for sediment erosion and accretion as suggested in previous studies [32] and more recently Dai *et al.,* [33]. According to these authors, values lesser than one suggest accretion, and vice versa, and the larger sediment accumulation rates yields to lower ratio of ^{226}Ra/^{228}Ra in surface sediment.

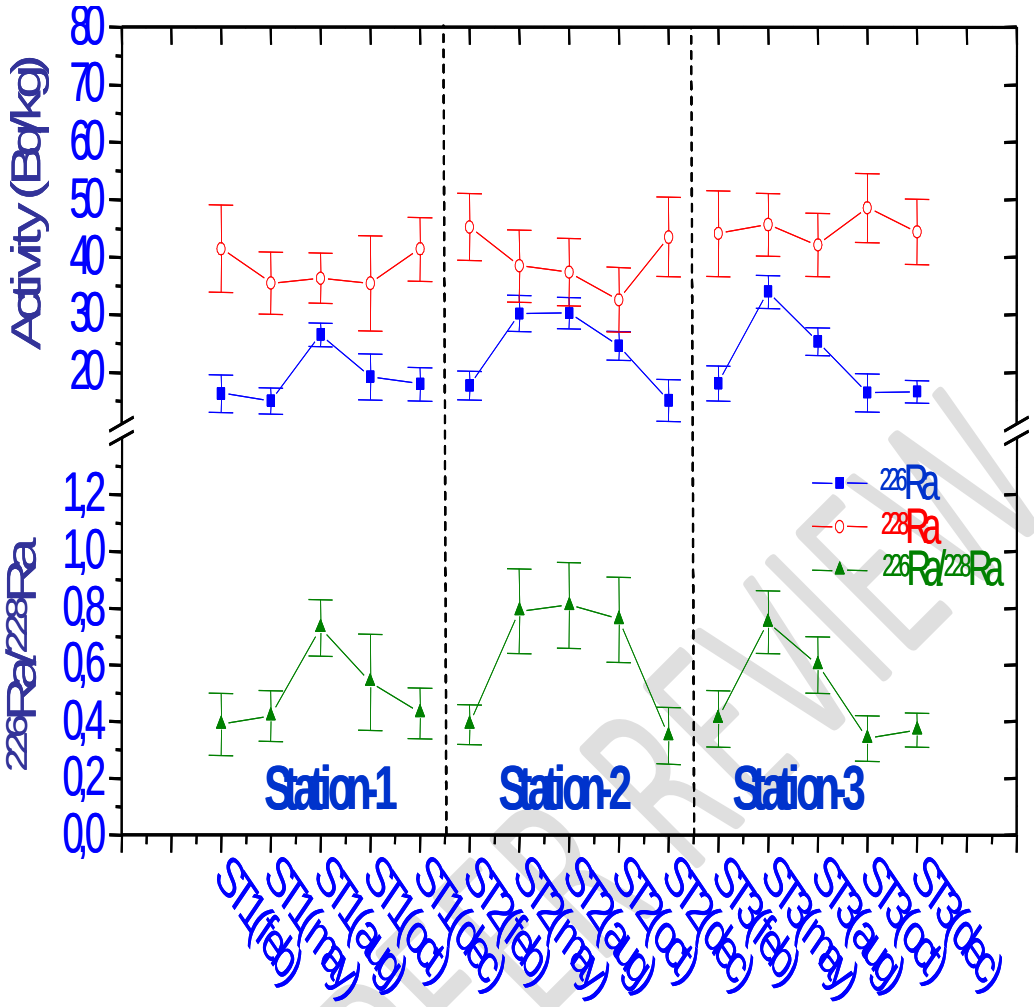

Fig. 4: Temporal Trends of ^{226}Ra and ^{228}Ra in surface sediments. Activities are in Bq.kg^{-1} dry weight and uncertainties are 1-σ statistical errors.

The values found in this study are all less than the unity ranging from 0.3 to 0.8, suggesting accretion and that the three studied sites were sedimentation zones with different sedimentation regimes. The result is in conformity with that of Dublin-Green [34] where a net accretion was reported to be occurring in the upper Bonny Estuary using the distribution pattern of skewness and kurtosis. In addition, the highest values (lowest accumulation) registered during the rainy months attributable to two possible effects: desorption of ^{228}Ra to less contaminated water and, in minor extent, relatively strong water turbulence that reduced the settling of fine particles.

ii. Temporal Distribution of Total ^{210}Pb in Surface Sediment

Total ^{210}Pb in surface samples collected for more than one year was determined via its daughter ^{210}Po by alpha spectrometry, which assumed that the secular equilibrium between both radionuclides was achieved. Specific activities corrected to the sampling dates are plotted in Figure 5. The activities in Station 3 (79 Bq.kg^{-1} dw,73 Bq.kg^{-1} dw and 56 Bq.kg^{-1} dw) were found to be lower than those in Station 1(121 Bq.kg^{-1} dw,120 Bq.kg^{-1} dw and 131 Bq.kg^{-1} dw),with Station 2 (92 Bq.kg^{-1} dw , 116 Bq.kg^{-1} dw and 128 Bq.kg^{-1} dw) having the lowest activity (56 Bq.kg^{-1} dw) registered in the sample collected in December (dry month). The unsupported component of ^{210}Pb in estuarine sediment had two sources: the atmospheric, which should be the same for the three stations due to their proximity to each other, and sedimentation of ^{210}Pb adsorbed onto particles delivered by the river inputs and/or dredging activities. As a result, low sedimentation rate in **St-3** could be behind the low ^{210}Pb specific activities in surface sediment.

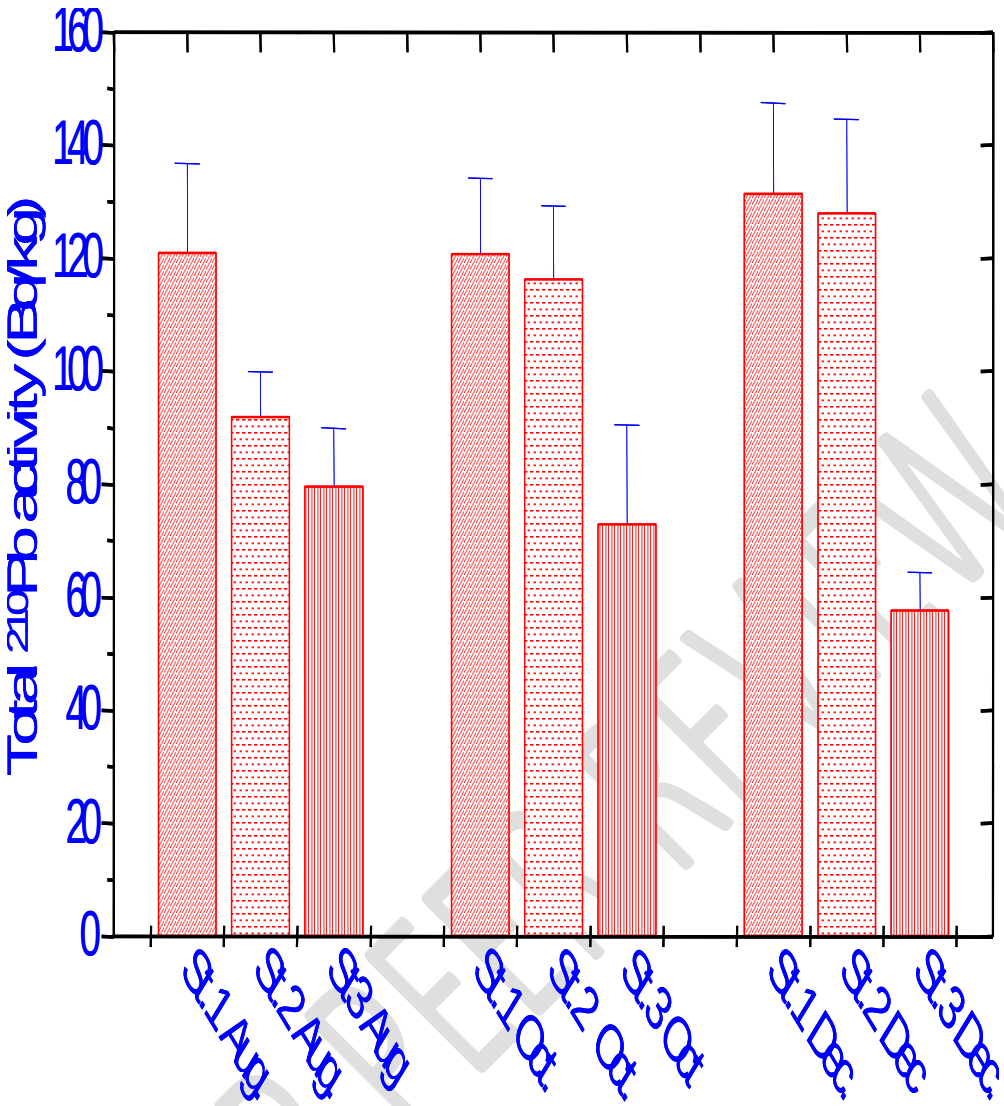

Fig. 5: Temporal distribution of total ^{210}Pb (Bq.kg^{-1}, dry weight) in surface Sediment

iii. Vertical Distribution of Radionuclides

The specific activities of ^{228}Ac (^{228}Ra), ^{212}Pb (^{228}Th) and ^{40}K against depth in the sampled sediments are plotted in figure 6. It was observed that ^{228}Th and ^{228}Ra activities were almost equal to one another at each layer (^{228}Th/^{228}Ra activity ratios ranged from 0.95 ± 0.08 to 1.02 ± 0.08 for **St-1**, from 0.86 ± 0.17 to 1.02 ± 0.19 for **St-2** and from 0.94 ± 10.12 to 1.01 ± 0.16 for **St-3** while ^{40}K values ranged from > 210.38 ± 56.78 to < 496.7 ± 33.45 for stations **1**, **2** and **3** respectively. In addition, the values obtained for organic matter ranged from 24.6 to 25.8%; 25 to 27.6% and 22 to 8% for stations **1**, **2** and **3** respectively.

The profiles displayed fairly homogenous distributions throughout the cores with the only exception being ^{40}K in **St-3**. A relatively visible increase of this radionuclide concentration in the basal 6-cm interval of the core was observed. The enhancement of ^{40}K may be attributed to the differences in the origin of the particles present in the deepest layers of the core that thus may contain more fine-grained clay sediments than the rest of the core. Vertical distributions of organic matter content were also depicted in Figure 6 for each coring site.

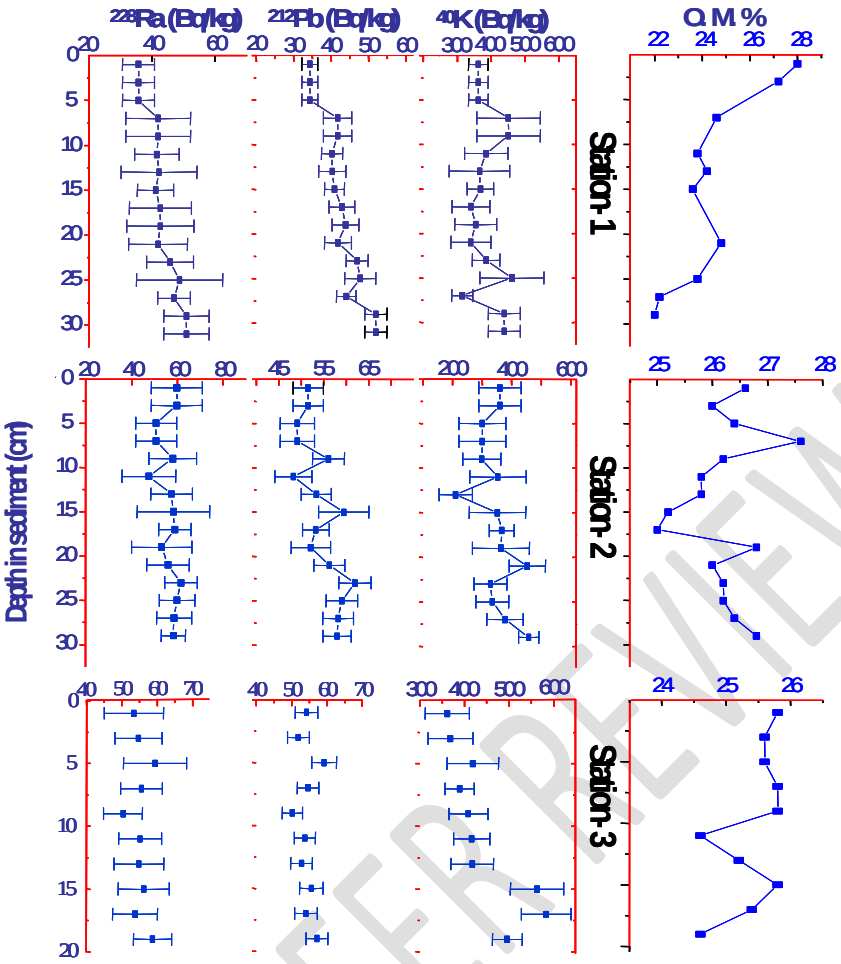

Fig. 6: Vertical distributions of ^{228}Ra, ^{212}Pb and ^{40}K in the three sampled sediment cores. Activities are in Bq.kg^{-1} dry weight and errors are 1-σ statistical uncertainties

^{40}K is a radionuclide, which is indicative of presence of fine-grained clay sediments in harbour and channel environments [35]. The values of ^{40}K found in the core samples collected at different months ranged between 264 and 462 Bq.kg^{-1} dry weight; displaying moderate variability among various months and stations. The values were within the range of values found in coastal environments worldwide [36]. The average specific activities over various months were 388 ± 89 Bq.kg^{-1} for **St-2** and **St-3**, and 326 ± 90 Bq.kg^{-1} for **St-1**. Therefore, no significant enhanced concentrations were recorded within the error margins of the radionuclide that could identify preferential sites and/or months for deposition of particles.

iv. Profiles of Radionuclides in the Sediment Cores

The total ^{210}Pb and ^{226}Ra activities in the three cores are presented in Figure 7 below. The vertical distribution for the Station **1** has values ranging from > 103.1 ± 6.94 to < 172.1 ± 11.26Bq.kg^{-1} dry weight, > 16.70± 3.12 and < 29.69 ± 4.86 Bq.kg^{-1} dry weight for total ^{210}Pb and ^{226}Ra respectively. In Station **2,** they ranged from > 70.38 ±3.15 to < 99.74 ± 4.87 Bq.kg^{-1} dry weight for both total ^{210}Pb and ^{226}Ra. The values recorded for the unsupported lead-210 (^{210}Pb$_{xs}$) ranged from > 80.65±8.09 to < 153.64 ± 12.80 and > 45.18±5.32 to < 75.31±6.54 Bq.kg^{-1} dry weight for Stations **1** and **2** respectively.

Furthermore, total ^{210}Pb and ^{226}Ra activities for Station **3** ranged from > 28.59±1.45 to < 93.99 ± 4.58, and >18.92 ± 2.36 to < 44.54 ± 3.06 Bq.kg^{-1} dry weight for total ^{210}Pb and ^{226}Ra respectively. The values for ^{210}Pb$_{xs}$ ranged from >10.65 ± 3.28 to < 66.99 ± 4.99 Bq.kg^{-1} dry weight at 0-12cm depth interval.

In addition, the total inventory (the sum of the product of activity, bulk density and thickness of each section) estimated were 22224, 10480 and 1597± 82 Bq.m^{-2} for Stations **1**, **2** and **3** respectively.

The total ^{210}Pb and ^{226}Ra activities throughout the three sediment cores were determined (Figure 7) with the purpose of carrying out radiometric dating. The vertical distributions corresponding to Stations **1** and **2** did not exhibit significant decrease in ^{210}Pb with depth but rather relatively constant activities with discrete maxima and minima. Unsupported lead-210 ($^{210}Pb_{xs}$) obtained by subtracting on a layer-by-layer basis the supported fraction (in equilibrium with ^{226}Ra) presented the same trends of variation as total ^{210}Pb and did not drop to zero in the basal layers. Therefore, these sediment cores (St-1 and St-2) were qualified as incomplete and disturbed, and were excluded from calculations of sedimentation rates, ages and total inventories of $^{210}Pb_{xs}$.

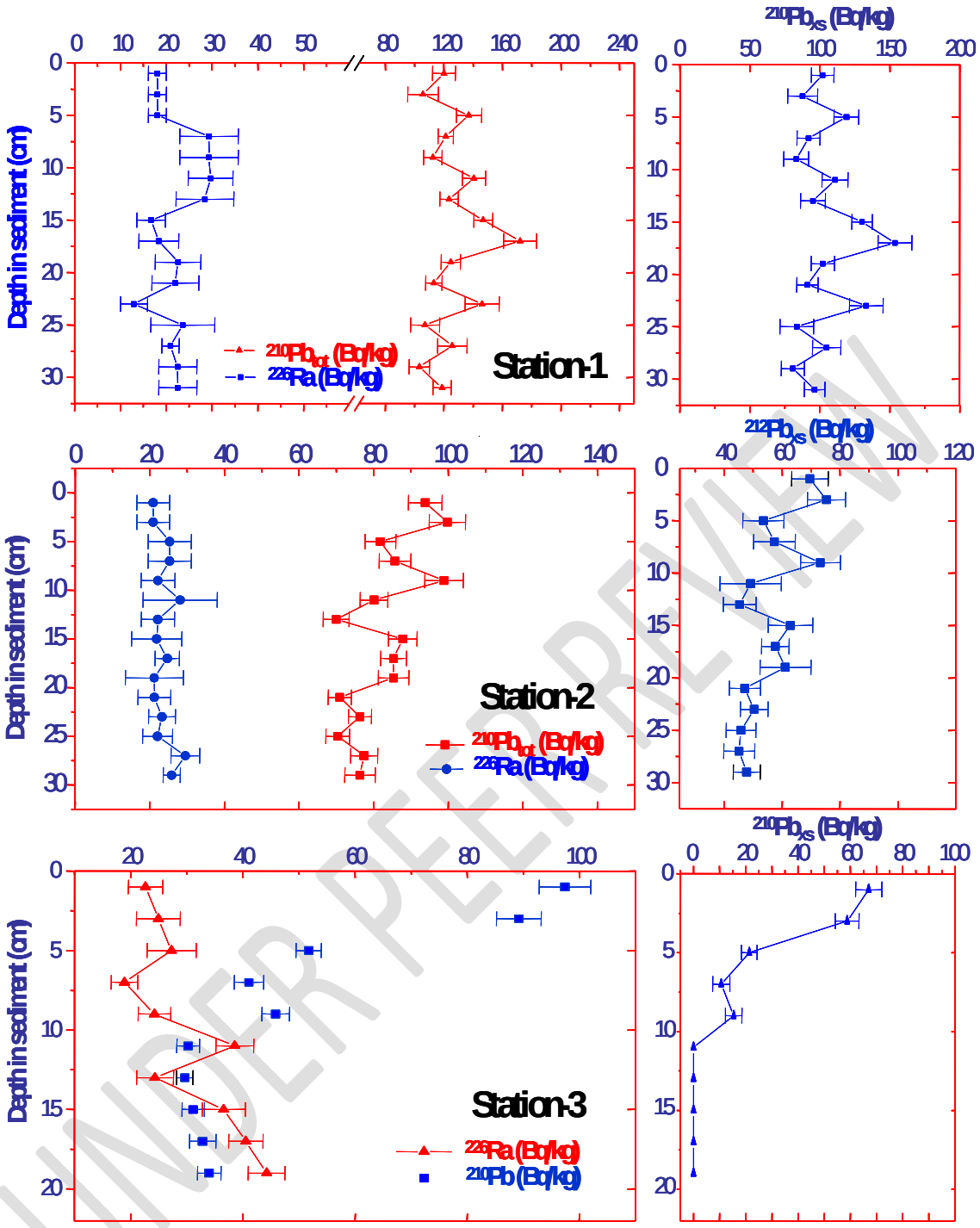

Fig 7: ^{226}Ra, total ^{210}Pb and $^{210}Pb_{xs}$ activity profiles in the sediment cores collected from the Bonny Estuary. Activities with 1-σ statistical errors are all in $Bq.kg^{-1}$ dry weight

On the other hand, ^{226}Ra at Station **3** showed an atypical distribution with depth especially at 10-12 cm depth interval, and the three basal layers where the corresponding activities exceeded unexpectedly total ^{210}Pb. Such behaviour ($^{226}Ra > {}^{210}Pb$) was observed in other environments but in the upper core layers [37], which introduced difficulties in estimating unsupported ^{210}Pb. This disequilibrium could be partially correlated to the organic matter content (OMC plotted in Figure 6) in these layers since ^{226}Ra activity increased as OMC decreased, but evidently the profiles at Stations 1 and 2 did not exhibit any pattern of variation with OMC, which made this assumption quite questionable.

With respect to the profile obtained in the sediment core collected at Station **3**, a special assumption was made in an attempt to apply conventional dating models. As total ^{210}Pb activity in the bottom 10-cm depth interval of the sediment core was rather constant, it was assumed that the corresponding activity matched the fraction of supported ^{210}Pb, which was supposed to be constant throughout the core depth [8]. Thus, the average activity of the five down-core layers was subtracted from the measured total ^{210}Pb activity at each depth in the core to obtain the excess ^{210}Pb profile plotted in Figure 7.

The total inventory (the sum of the product of activity, bulk density and thickness of each section) was 1597 ± 82 Bq.m^{-2}, which was much lower than the partial inventories for Stations 1 and 2 sediment cores (>22224 Bq.m^{-2} for St-1 and >10480 for St-2). These differences in inventories from one site to another could be attributed to horizontal transport within the estuary and, in major extent, to the variability in sedimentation rates at specific sites [38]. Only a small fraction of atmospherically derived ^{210}Pb was deposited with particles at Station **3**. The annual flux of $^{210}Pb_{xs}$ onto sediment at Station **3**, calculated as the product of λ, the decay constant of ^{210}Pb, and the total inventory was 49.6 ± 2.5 Bq.m^{-2}.y^{-1}. The unsupported ^{210}Pb has been widely and successfully used as a chronometer in sediment geochronological studies [39].

The CSR (Constant rate of supply) model and CIC (Constant Initial Concentration) model were applied to the $^{210}Pb_{xs}$ profile of the core collected at Station **3**. Both models assumed that the input of atmospherically derived ^{210}Pb at a given location is quite uniform over a period of time; or at least close enough to the age of the core. Although $^{210}Pb_{xs}$ activities were different from the values gotten from the least-square fitting when using CIC model, the average sedimentation rate throughout the core obtained from CRS model (0.068 ± 0.015 g.cm^{-2}.y^{-1}) was almost the same to that obtained from CIC model, which was 0.065 ± 0.004. However, the estimated ages were quite different for some layers.

v. Ages, Sedimentation Rates and Depth Relationships

The ages and sedimentation rates obtained from the Constant Rate of Supply (CRS) model at each stratigraphic level are displayed in Figure 8. The values of 0.074 g.cm^{-2}.y^{-1}, 0.109g.cm^{-2}.y^{-1}, 0.039g.cm^{-2}.y^{-1}, 0.550g.cm^{-2}.y^{-1} and 0.064g.cm^{-2}.y^{-1} were obtained as sedimentation rates corresponding with year 2004, 1997, 1973, 1955 and 1943. Although $^{210}Pb_{xs}$ activities are different from the various values provided by the least-square fitting when using Constant Initial Concentration (CIC) model. The average sedimentation rate throughout the core obtained from CRS model (0.068 ± 0.015g.cm^{-2}.y^{-1}) was nearly the same as that obtained from the CIC model (0.065 ± 0.004), but the estimated ages were quite different for some stratigraphic layers.

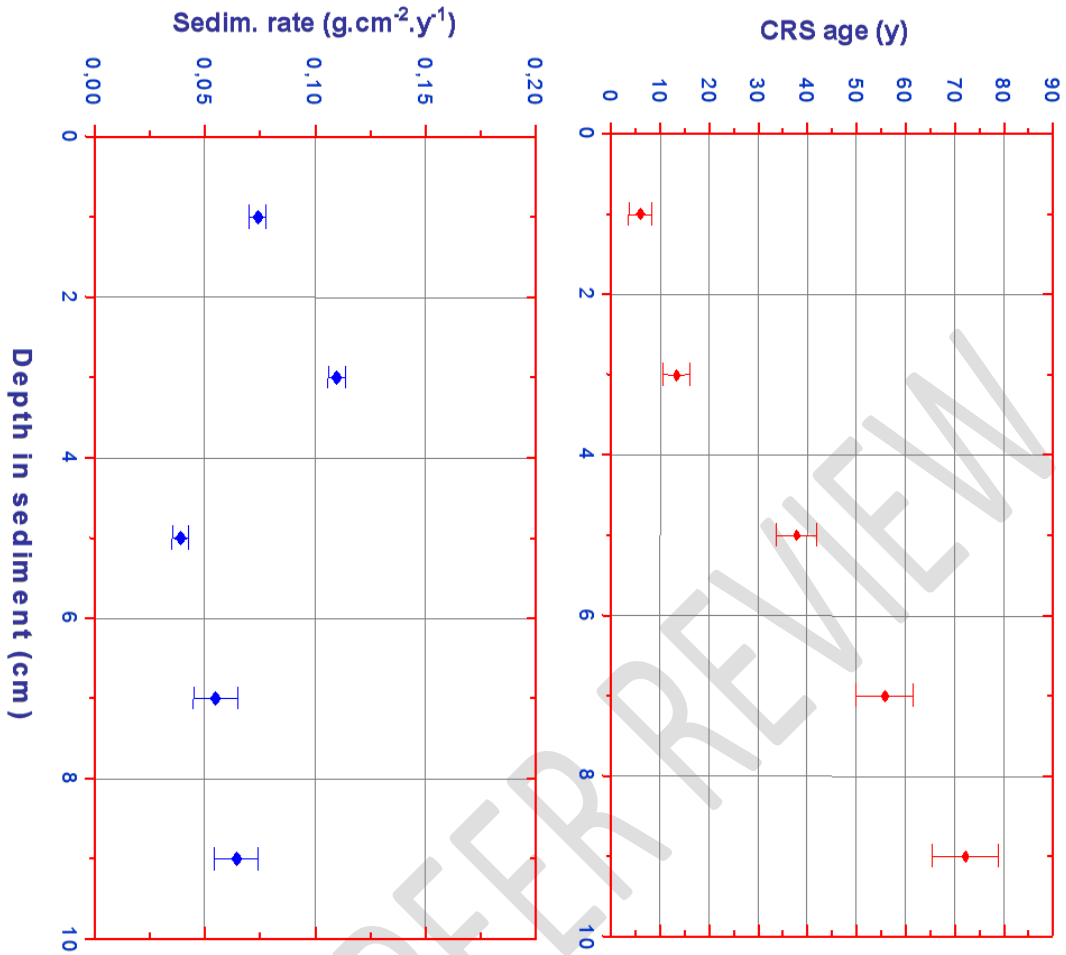

Fig. 8: Age versus Depth; Sedimentation Rate versus Depth relationships determined by CRS Model for the sediment core at Station **3**

The sedimentation rates calculated suggested low sedimentation which has earlier been reported to signify a very calm environment according to Dublin-Green [34]. It has been reported that the shallow marginal area of the Bonny Estuary is a low energy environment characterized by weak tidal currents (current velocity in the low marginal area is between 20-30cm/sec during flood tide), which promotes the deposition of fine sediments while the deeper channel centres are areas of scourging dominated by strong tidal currents. Values obtained were also in agreement with the observation made during sampling where the flow of the water was seen to be calm and parallel (laminar flow) which is associated with quite environment.

vi. Validation of ^{210}Pb Ages using ^{137}Cs

^{210}Pb chronology was confirmed by a second independent tracer (^{137}Cs). ^{137}Cs in the sub-samples of the core collected at Station **3**. The results are presented in Table 1and values range from below to slightly above the limit of detection by the HPGe gamma spectrometer with 70% relative efficiency.

Cesium-137, which is an artificial radionuclide resulting from nuclear bomb testing and detonations since early 1950's, was the tracer of choice to identify the period of maximum atmospheric fallout. However, deposition of this radionuclide has been recognized through comprehensive compilation of its global fallout to be different in the northern and southern hemispheres [40]. It was expected therefore, that ^{137}Cs specific activities (Table 1) in our sediment samples from the Bonny Estuary,

being a tropical area, would be relatively low. Effectively, ^{137}Cs in the sub-samples of the core collected at Station **3** as shown in Table 1, were below or slightly above the limit of detection of our detection system (HPGe gamma spectrometer with 70% relative efficiency). Nevertheless, based on the CRS ages, the period of maximum fallout (1963) should be at 6-8-cm depth intervals in the core. The measured activity within this depth interval was 1.416 ± 0,112 Bq.kg^{-1}, and higher than the activity immediately below the 6-8-cm depth intervals (i.e. from 8-10-cm), which was < LD = 1.24 Bq.kg^{-1}.

It should be considered that the activity measured within the 6-8-cm depth interval is the mean value of activities of a number of thin layers formed during a period of about 15 years according to the CRS model. Thus, the 2-cm thickness is itself a layered structure due to the low sedimentation rate (0.124 cm.y^{-1}).Thus, the maximum activity corresponding to 1963 is diluted in the surrounding sediment of relatively low ^{137}Cs content. On the other hand, activities of the upper stratigraphic intervals (0-2cm, 2-4cm and 4-6cm) were both undetectable due to the low amount of materials analysed. The corresponding limits of detection were higher than the specific activity of 6-8cm depth interval. This, in addition to the low core resolution (within 2cm depth interval), introduced serious difficulties in identifying the depth of the peak associated with the atmospheric weapons testing period. Nevertheless, ^{137}Cs activities measured individually in the basal 10cm depth interval of the core were all below LD = 1.20 Bq.kg^{-1}, and less than 0.70 Bq.kg^{-1} when combined all together.

Such discovery assumed that sediment cores below 10cm depth interval in Station **3**, where no ^{137}Cs activity was observed (probably deposited before the beginning of the periods of nuclear detonations) is in perfect agreement with CRS ages before 1940. If there was any ^{137}Cs in these layers, it would have been explained by one or a combination of two factors: firstly, ^{137}Cs desorption from the overlaying sediment and its subsequent diffusion into the deeper stratigraphic intervals. The distribution coefficient of Cs is about two to three orders of magnitude lesser than that of highly reactive particles such as Pu and Am [41].Secondly, ^{137}Cs possible cross contamination among layers during coring operation. The presence of high levels of ^{226}Ra, exceeding total ^{210}Pb (Figure 5), and ^{40}K (Figure 4) may be attributed to the massive upward migration of Ra-enriched particles with formation water during oil exploration and production [42], which began in early 1900. Diffusion of these radionuclides into the sediment column cannot be behind their enhancement in deeper stratigraphic layers since the capacity of their penetration in sedimentary systems is very limited as reported by [43].

Table 1: Validation of ^{210}Pb Ages using ^{137}Cs (^{137}Cs activities in Bq.kg^{-1} dry weight in the sampled core collected at Station 3 (LD is limit of detection). Sample depth of 10-20cm was obtained by combining all sub-samples of 2cm thickness

Layer (cm)	Year	^{137}Cs Act. (Bq.kg^{-1})	LD (Bq.kg^{-1})
0−2	2004	<LD	1.496
2−4	1997	<LD	1,521
4−6	1973	<LD	1,825
6−8	1955	1,416 ± 0,112	--
8−10	1938	<LD	1,240
10−20		<LD	0.702

4. CONCLUSION

The research evaluated temporal trends of naturally occurring radionuclides and their vertical distributions in sediment cores collected from three sites of diverse sedimentation regimes in Bonny Estuary, developed and implemented sediment dating with unsupported lead-210, assessed degree of catchment disturbance in the area by comparing recent sedimentation rates with the pre-European sedimentation rates.

The temporal variations of Ra isotopes showed a fairly uniform distribution among all sampled locations in each month with ^{228}Ra, while ^{226}Ra displayed some variability with generally lower specific activities in dry months than in rainy months. The values found in the study were all less than unity ranging from 0.3 to 0.8, which suggested sediment accretion and that the study area corresponded to zones with different sedimentation regimes. The result is in conformity with that of Dublin-Green [34] where a net accretion was reported to be occurring in the upper Bonny Estuary using the distribution pattern of skewness and kurtosis.

Temporal distribution of total ^{210}Pb in surface samples determined via its daughter ^{210}Po by alpha spectrometry assumed that the secular equilibrium between both radionuclides was achieved. However, the activities in Station 3 were found to be lower than those in Station 1, with Station 2 having the lowest activity registered in the samples collected in December month. The specific activities of ^{228}Ac (^{228}Ra), ^{212}Pb (^{228}Th) and ^{40}K against depth in the sampled cores were observed to be almost equal to one another at each stratigraphic interval. The profiles displayed fairly homogenous distributions throughout the cores with the only exception being ^{40}K in Station 3, which may be attributed to the differences in the origin of the particles present in the deepest layers of the sediment core.

The average sedimentation rate throughout the core obtained from Constant Rate of Supply model ($0.068 \pm 0.015 g.cm^{-2}.y^{-1}$) was nearly the same as that obtained from the Constant Initial Concentration model (0.065 ±0.004). However, the estimated ages were quite variable with depths of various stratigraphic layers. The age of the sediment core was dated approximately 80 years, which was qualitatively validated using ^{137}CS whose activity was definitely undetected in the basal part of the

core.The sedimentation rates calculated suggested low sedimentation characterized by low energy environment dominated by weak tidal currents.

REFERENCES

Ajayi, T.R; N. Torto; P.T. Chokossa; and A. Akinlua. “Natural Radioactivity and Trace Metals in Crude Oil: Implication for Health”. *Environ Geochem Health*, 2009; 31**:** 61-6

Mokobia C.E. “Effect of Gamma Irradiation on the Grain yield of Nigerian *Zea mays* and *Arachis hypogaea”.J. Radiol. Prot.* 2006; 26: 423.

3. El-Daoushy, F. “Radioactivity Acrosols in the Lower Atmosphere”. (In:Masuda, S., Takashi, K. (Eds.), *Aerosols: Industry, Health and Environment*, 1988; 2:217-221

4. Appleby, P. G. “Chronostatigraphic Techniques in Recent Sediment” In: Last W.M. and Smol J.P eds, *tracking Environment Change Using Lake Sediment, Vol. 1, Basin Analysis, Coring and Chronological Techniques,* Kluwer Academic Publishers, Dordrecht, The Netherlands, 2001; 171-203

5. Goldberg, E.D. “Geochronology with ^{210} Pb”. (In: *Radioactive dating, International Atomic Energy Agency, Vienna*). 1963; 121-130.

6. Eakins J.D and Morrison R.T. “A New Procedure for the Determination of lead-210 in Lake and Marine Sediment”. *Int.J. Appl. Radiat.* 1978; 29:531-536

7. Appleby, P. G; P.J Nolan; D.W.G. Ifford; M.J.G Odfrey; F. Oldfield; N.J. Anderson; and R.W. Battarbee. “^{210}Pb Dating by Low Background Gamma Counting in Nigeria”. *African J. Environm. Pollut. Health* 1986; 4 (1): 26-32.

8. Schelske, C.L; A. PeploW; M. Brenner; and N. Craig. “Spencer Low-Background Gamma Counting: Applications for ^{210}Pb Dating of Sediments”. *Journal of Pale limnology* 1994; 10**:** 115-128.

9. Appleby, P.G. and Oldfield, F. “Application of 210-lead to Sedimentation Studies”. In: Ivanovich, M., Harmon, R.S. (Eds.), *Uranium Series Disequilibrium: Applications to Earth, Marine and Environmental Sciences* second ed. Oxford Science. Oxford, 1983; 731-783.

Robbins, J.A. and Herche, L.R. “Radiochemical Limnology: Models and uncertainty in ^{210}Pb dating of sediments”. *Verh. Internat. Verein*. *Limnol.* 1993; 25:217-222

George, C. F., University of Aberdeen., & Petroleum Technology Development Fund (Nigeria). *Geometries of surface and subsurface landforms and deposits in the Niger Delta*. 2014.

Asseez, L.O. *“Review of the Stratigraphy, Sedimentation and structure of the Niger Delta in geology of Nigeria”*. Elizabethan Publishing Co., Lagos, Nigeria. 1976.

Adeniyi, H.A. and Mbagwu, J.G. “The Assessment of Water Quality of the Jakara Reservoir in Kano State”. *Ann. Rep. Nat. Inst. Freshwater Fish*. Res. Nig., 1983; 89: 136-139.

Reijers, T.J.A. Stratigraphy and Sedimentology of the Niger Delta. *Geologos*, 2011;17(3), 133-162.

NEDECO. “The Waters of the Western Niger Delta”. Report on an Investigation. 1961.

Ofomata, G. E. K. *Nigeria in Maps: Eastern States.* Ethiope *Publishing House, Benin City.* 1975.

Pillay, K.K.S; C.C.J. Thomas; and J.A. Sandel. “Activation Analysis of Airborne Selenium as a Possible Indicator of Atmospheric Sulphur Pollutant”. *Environ Sci Technol* 1973; *5:747*

Abam, T.K.S. “Impact of Dams on the Hydrology of the Niger Delta”*. Bull. Int. Assoc. Engni Geol. & Environ*. 2001; 57: 239-251.

Abam, T.K.S. and Beets, C. *Coastal Zone Management Strategy for Hooding and Erosion in the Niger Delta*. *A Report Prepared for the World Bank,* 1995.

Walling, G.A; P.M. Visscher; A.D.Wilson; B.L. Meteir; G. Simm, and S.C Bishop. "Mapping of Quantitative Trait Loci for Growth and Carcase Traits in Commercial Sheep Population". *J. Anim. Sci.* 2004; 82: 22-35

Widdows, J. and Brinsley, M.D. "Impact of Biotic and Abiotic Processes on Sediment Dynamics and the Consequences to the Structure and Functioning of the Intertidal Zone". *J. Sea Res*. 2002; 48: 143-156.

2 Jie, H; Z. Zhinan; Y. Zishan; and J. Widdows. "Differences in the Benthic pelagic Particle Flux (biodeposition and sediment erosion) at Intertidal Sites with and without Clam (*Ruditapes philippinarum*) Cultivation in Eastern China". *J. Exp.Mar. Biol. Ecol.* 2001; 261**:** 245-261.

. Graf, G. and Rosenberg, R. "Biosuspension and Biodeposition": A Review. *J. Marine Syst*. 1997; 11: 269-278.

. Black, K.S; T.J.Tolhurst; D.M. Paterson; and S.E. Hagerthey. "Working with Natural Cohesive Sediments". *J. Hydol. Eng.* 2002; 128: 2-8.

. Andersen, T.J; K.T Jensen; L.C Lund-Hansen; K.N. Mourtisen; and M. Pejrup."Enhanced Erodability of Fine-grained Marine Sediments". *Hydrobia ulvae*. *J. Sea. Res.* 2005; 48: 51-58.

Goudie, A. and Middleton N.J. "Sahara Dust Stoms: Nature and Consequences" *Earth-Sci. Rev*. 2001; 56: 179

Ibe, A.C. "*Coastline Erosion in Nigeria"*. Ibadan University Press, Ibadan Nigeria, 1986.

. Brenner, M; C.L. Schelske; and L.W. Keenan. "Historical Rates of Sediment Accumulation and Nutrient Burial in Marshes of the Upper St. Johns River Basin, Florida, USA". *J.Paleolimnol.* 2001; 26: 241–257.

2. Muller, G. "Index of Geo-accumulation in Sediments of the Rhine River". *Geo. J.,* 1969; 2(3): 108-118.

. Turekian, K.K. and Wedepoi, K.H. "Distribution of Element in Some Major Units of the Earth's Crust*". Geol. Soc. Am. Bull*. 1961; 72: 175-192.

. Elsingep, R. J. and Moore, W. S. "^{226}Ra and ^{228}Ra in the Mixing Zones of the Pee Dee River-Winyah Bay, Yangtze River and Delaware Bay Estuaries". *Estuar. Coast. Shelf Sci*, 1984; 18: 601-613.

. Bai, Z.G., Wan, G.J. and Wang, C.S. "Geochemical Speciation of Soil ^{7}Be, ^{137}Cs, ^{226}Ra, ^{228}Ra as Tracers to Particle Transport". *Pedosphere.* 1997; 7(3): 263–268.

33. Dai, A. Characteristics and trends in various forms of the Palmer Drought Severity Index during 1900. 2008. *J. Geophys. Res. Atmos.* 2011; *116*(D12).

3. Dublin-Green, C.O. "Some Textural Characteristics and Organic Matter Contents of Recent Sediments in the Bonny Estuary, Niger Delta". *Technical Paper.* 1985; *N° 67*. ISBN: 978-2345-069.

35. Noakes, S. "Post Disposal Areal Mapping of Sediment Chemistry at the Fort Pierce, Florida ODMDS". *U.S. Environmental Protection Agency, Final Report*. 2003.

36. UNSCEAR. "Sources, Effects and Risks of Ionizing Radiation". Report to the General Assembly (New York: United Nations). 2000; 65

37. Brenner, M., Peplow, A. J., & Schelske, C. L. Disequilibrium between ^{226}Ra and supported ^{210}Pb in a sediment core from a shallow Florida lake. *Limnol. Oceanogr.* 1994; *39*(5), 1222-1227.

38. Heltz, G.R; G.H. Setlock; A.Y. Cantillo; and W.S. Moore. “Processes Controlling the Regional Distribution of ^{210}Pb, ^{226}Ra and Anthropogenic Zinc in Estuarine Sediments”. *Earth & Planet. Sci. Let*. 1985; 76**:** 23-34.

. Laissaoui, A; M. Benmansour; N. Ziad; M. IbnMajah; J. M. Abril; and S. Mulsow. “Anthropogenic Radionuclides in the Water Column and a Sediment Core from the Alboran Sea”: Application to Radiometric Dating and Reconstruction of Historical Water Column Radionuclide Concentration. *J. Paleolimnol*. 2008; 40(3), 823-833.

4. Pfitzner, J; G. Brunskill; and I. Zagorskis. “^{137}Cs and excess ^{210}Pb Deposition Patterns in Estuarine and Marine Sediment in the Central Region of the Great Barrier Reef Lagoon, North-eastern Australia”. *J. Environ. Radioact*. 2004; 76: 81–102.

4. International Atomic Energy Agency. “Sediment Distribution Coefficients and Concentration Factors for Biota in the Marine Environment”. *Technical Reports Series.* 2004; ISSN 0074–1914; no. 422.

4 Kolb, W.A. and Wojcik, M. ‘Enhanced Radioactivity Due to Natural Oil and Gas Production and Related Radiological Problems”. *Sci. Total Environ.* 1985; 45**:** 77–84.

4. Ligero, R. A; F. Feria; M. Casas-Ruiz; and C. Corredor. Diffusion of ^{226}Ra and ^{40}K Radionuclides Reproduced in Underwater Sedimentary Columns in Laboratory. *J. Environ. Radioact.* 2006; 87**:** 325-334.